Available online at www.sciencedirect.com

SciVerse ScienceDirect

Ceramics International 39 (2013) 7613–7618

CERAMICS INTERNATIONAL

www.elsevier.com/locate/ceramint

Preparation and dielectric properties of dense and amorphous alumina film by sol–gel technology

Baofu Hu[a,b], Manwen Yao[a,*], Pengfei Yang[a], Wei Shan[a], Xi Yao[a]

[a]*Functional Materials Research Laboratory, Tongji University, China*
[b]*College of Physics and Chemistry, Henan Polytech University, China*

Received 16 November 2012; received in revised form 4 March 2013; accepted 5 March 2013
Available online 14 March 2013

Abstract

Dense and crack-free aluminum oxide films were fabricated by sol–gel spin-coating technology. Aluminum nitrate ($Al(NO_3)_3.9H_2O$) was used as the precursor material. X-ray diffraction shows that the fabricated films are amorphous. X-ray photoelectron spectroscopy confirms that the thin films are alumina (Al_2O_3). Field-emission scanning electron microscopy images of the films reveal that the films are compact with a dense cross section. Dielectric measurements were carried out on samples with a metal–insulator–metal structure. The electrical characteristics of the films were affected by the thermal sintering temperature of the films. The leakage current density of the films decreases with the increase in the sintering temperature and increases with the increase in the measuring temperature. The leakage current shows a linear dependence on the voltage in the low-electric field-regime. The current density ascends to higher values due to the effect of space charges in the high-electric-field regime. The ionization energy of the top-electrode metals (Au, Pt or Ti–Au) has a strong effect on the leakage current.

Keywords: A. Sol–gel processes; C. Electrical properties; D. Al_2O_3

1. Introduction

Alumina has long been known as a high performance ceramic. The mechanical strength [1], hardness, abrasive resistance and chemical resistance [2] of the material are all high among advanced ceramics. The low dielectric loss in the microwave band combined with its high resistivity have rendered the alumina ceramic popular as a high-end material for microwave device substrates and semiconductor integrated circuit packaging, which are difficult to replace with other materials [3,4]. Alumina films have also been widely used in chemical engineering and other technological fields as catalyst carriers, ultra-filtration and separation films as well as abrasive-resistant and optical coatings [5,6]. In many of the above applications, the preparation of alumina film with porous and meso-porous structures is the main concern [7,8]. The high electrical breakdown strength of alumina thin films has recently drawn our attention to explore their potential application as dielectric films with high energy storage density. High energy storage density is currently one of the critical issues facing the development of low-carbon and green energy technology. For energy storage purposes, high dielectric breakdown strength and low conductivity are the major concerns. To achieve better performances, the preparation of dense alumina films is very important. However, there is not much research on the preparation and dielectric behavior of dense alumina films reported in the literature.

There are many physical and chemical approaches to prepare alumina films, such as pulse laser deposition [9], chemical vapor deposition [10,11], spray pyrolysis [12], sputtering [13] and sol–gel processing [14–16]. Among these techniques, the sol–gel method is an emerging route that can be used to easily deposit thin films on different types of substrates and prepare alumina coatings on ceramic powders with various particle sizes of at an industrial scale. Hence, the sol–gel preparation of alumina films was the primary focus of our study.

It is well known for a long time that the anodized aluminum film treated in liquid electrolyte under a DC formation voltage is able to withstand very high applied voltages, which are widely used to make various electrolytic capacitors for electronic industry. However, the structure of the anodized aluminum oxide films is very complicated. The films were grown in a complicated

*Corresponding author. Tel.: 86 21 65983130.
E-mail address: yaomw@tongji.edu.cn (M. Yao).

0272-8842/$ - see front matter © 2013 Elsevier Ltd and Techna Group S.r.l. All rights reserved.
http://dx.doi.org/10.1016/j.ceramint.2013.03.016

wet chemistry environment. The OH^- radical from water and the anion radicals from the electrolytes would penetrate into the structure under the DC formation voltage. The structure of such film in nano-meter scale is inhomogeneous. The detail complication of the structure has not yet been fully revealed. Although the chemical formula of aluminum oxide is quite simple, however the structures of its oxides are rather complicated. There are more than ten crystalline variants of aluminum oxide. The α-, β- and γ-Al_2O_3 are the most stable crystalline structures. The others are very much depending on their physical and chemical processing environments and are less encountered and less stable. From engineering point of view, the structure of such anodized aluminum film is widely referred as amorphous and/or γ-Al_2O_3 structure. In this work the major concerns are the electrical conduction under high field and the dielectric breakdown strength of the aluminum oxide film prepared from sol–gel process, which is another wet chemistry route to prepare the film in comparison with the anodized aluminum oxide film.

Though many studies on Al_2O_3 thin films have been published [17–19], only a few have been devoted to the dielectric properties of such films [20]. Many details regarding the dielectric characteristics of alumina films are not yet clear. The main objective of this work was to study the dielectric properties of Al_2O_3 thin films derived from an inorganic salt $Al(NO_3)_3$ solution by a sol–gel technique. The thin films were calcined at high temperatures ranging from 550 °C to 650 °C. Lower than the above temperature range, the sol–gel derived films are mostly in amorphous state. The current density of the thin films was measured in the temperature range from 25 °C to 150 °C. Three different metals were used as the top electrode. Herein, the dielectric properties of the Al_2O_3 thin films are discussed in detail.

2. Experimental

All chemicals used in this study were of reagent-grade purity and available commercially; they were used without further purification. The starting material used to prepare the films was $Al(NO_3)_3.9H_2O$. The material was dissolved in glacial acetic acid and stirred for 30 min. Then, acetylacetone was added to the solution as a chelating agent, and the solution was stirred for another 30 min. A small amount of polyvinyl alcohol (PVA) aqueous solution was added to the mixture solution as an anti-cracking agent. The mixture was then stirred for 6 h at room temperature. A clear and transparent pale-yellow sol was obtained. The concentration of $Al(NO_3)_3$ in the sol was 0.3 mol/l. Two kinds of substrates, silicon (Si) and platinized silicon (Pt/Ti/SiO_2/Si) wafers were used in this work. Before spin-coating the alumina precursor sol solution, the substrates were cleaned thoroughly by ultrasonication in acetone, ethanol and deionized water, successively, and then blow dried with N_2.

After aging for 3 days, the precursor was used to deposit films on the substrates by spin-coating at 3000 rpm for 20 s per layer in a clean-room environment. The same procedure was repeated many times until the desired thickness was reached. The gel films were calcined at 550 °C, 600 °C and 650 °C for 2 h in a muffle furnace in air to form alumina films.

The xerogel was examined by a thermal analysis instrument (NETZSCH STA449C). The crystal structure of the thin films was identified by X-ray diffractometry (BRUKRER D8 Advance Diffractometer). An X-ray photoelectron spectrometer (PHI-5000C ESCA system) was used to identify the chemical composition and binding states of the films. The morphology of the film was examined using a field-emission scanning electron microscope (FE-SEM, FEI Quanta 200 FEG). For electrical measurements, top electrode pads measuring 1 mm in diameter were sputtered through a shadow mask onto the Al_2O_3 thin films by DC sputtering. Leakage current–voltage (*J–E*) measurements were performed using a Keithley 2400 electrometer. The capacitance was measured using an Agilent 4284A LCR meter controlled by a computer.

3. Results and discussion

To identify the calcination temperature of the gel films, a thermal analysis of the xerogel was performed. The thermogravimetry (TG) curve is shown in Fig.1. The TG curve shows that there is no apparent mass change above 550 °C. This result indicates that the decomposition of the organic groups is completed below 550 °C. Thus, we decided to calcine the gel films at 550 °C, 600 °C, 650 °C.

The XRD spectra reveal that the films possessed a non-crystalline structure even after being calcined at 650 °C for 2 h. Fig.2 shows the XRD pattern of the Al_2O_3 thin film calcined at 650 °C. No apparent diffraction peaks can be identified from the pattern. Thus, it can be concluded that the films were amorphous [21].

The chemical composition and binding states of the alumina film calcined at 550 °C can be identified from the corresponding XPS spectrum. Fig. 3 is the XPS survey spectrum of the film deposited on a Si substrate calcined at 550 °C for 2 h. Except for a small amount of carbon, there are no other elements other than aluminum and oxygen. The carbon peak arises from an overlying contaminant hydrocarbon layer. The observed binding energy of aluminum is in good agreement with that reported in the literature for Al_2O_3 [5]. The deconvolution of the main peak corresponding to oxygen atoms in the XPS spectrum is shown in Fig. 4. Two peaks at 531.3 eV and 532.5 eV are identified. They correspond to the Al–O band [22,23] and H–O band [24], respectively, which indicates that the film may have adsorbed H_2O.

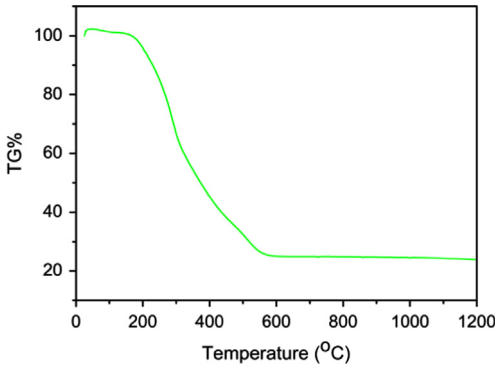

Fig. 1. Thermogravimetry (TG) curve of the alumina xerogel.

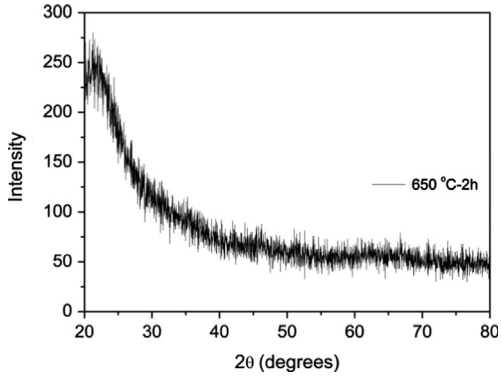

Fig. 2. XRD pattern of Al_2O_3 film on Si substrate calcined at 650 °C for 2 h.

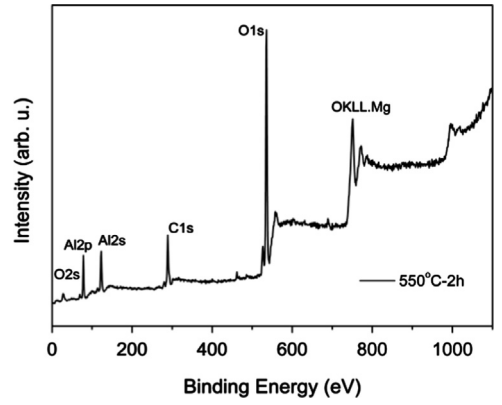

Fig. 3. XPS survey spectrum of an alumina film calcined at 550 °C for 2 h.

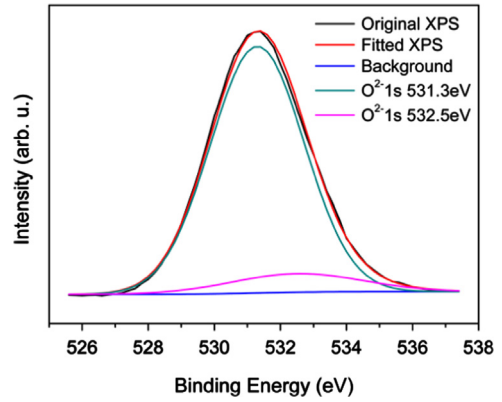

Fig. 4. Typical deconvolution of O1s main peak of the Al_2O_3 film.

Fig. 5 shows surface and cross-sectional FESEM micrographs of Al_2O_3 films deposited on Pt/Ti/SiO_2/Si substrates at various annealing temperatures. The films are dense and homogeneous. The films, calcined at 550 °C, do not show an apparent grain structure, suggesting that they are amorphous in structure. The film calcined at 600 °C, shows signs of the development of a nano-grain structure. After reaching the highest annealing temperature of 650 °C, the nano-grain structure becomes more and more apparent, which indicates that the films are gradually transitioning from an amorphous to a crystalline state with the increase in the annealing temperature, despite the fact that X-ray diffraction still indicates an amorphous structure.

It is well known that Al_2O_3 is an excellent dielectric material with very low leakage current characteristics. To measure the *J–E* characteristics of the films accurately, maintaining a reasonable voltage ramp rate during measurements is important. A ramp rate of 0.3 V/s was used in all of the measurements. Fig. 6 shows the typical *J–E* characteristics of the alumina films measured at room temperature. The figure shows that the leakage current density increases with the increase in the applied electric field. The leakage current of the thin film calcined at 600 °C is approximately 10^{-7} A cm^{-2} at 10 MV/m and increases to 10^{-5} A cm^{-2} at 120 MV/m. This result indicates that the films have good insulation behavior. The leakage current density decreases with the increase in the calcination temperature. The current value of the sample calcined at 650 °C is approximately one order of magnitude lower than that of the sample calcined at 550 °C. We believe that the decrease in current with the increase in the calcination temperature can be attributed to the gradual change in the amorphous structure toward a crystalline state, which may reduce the number of unoccupied cation sites of the alumina lattice [25].

Fig. 7 shows the *J–E* characteristics of the Al_2O_3 films measured at different temperatures and plotted on a ln(*J*)–ln(*E*) scale. Each curve can be separated into two sections fitted by two straight lines. For an electric field below 20 MV/m, the leakage current shows a linear dependence on voltage; the slope of the ln(*J*) vs. ln(*E*) curve is close to 1.0, indicating linear, Ohmic-like conduction. The electrons injected from the electrode at low electric fields are negligible. The leakage current is mainly attributed to thermally activated charge carriers. More thermally activated charge carriers are generated at higher temperatures. Hence, at these temperatures, the leakage current will be higher. When the electric field is higher than 20 MV/m, in addition to the thermally activated charge carriers, an increasing number of electrons will be injected into the film from the cathode with the increase in the electric field and form space charges. Some of the injected electrons will be captured by the traps of the film. Some of the injected electrons jump directly into the conduction band and participate in the conduction process; thus, the current density ascends to higher values. The slopes increase to 4.1, 3.3 and 2.5 at 25 °C, 80 °C and 150 °C respectively, which indicate that the current might be ruled by other conduction mechanisms at this electric field region.

Self-healing breakdown phenomena similar to those observed for semiconductor MOS devices were observed [26]. Current density spikes were consistently observed in the *J–E* plots, as shown in Fig. 6. Each spike signifies a local breakdown and self-healing event. For samples with gold as the top electrode, a sudden drop in the current density was observed at approximately 160 MV/m. Microscopy revealed that the local lift-off of the top gold electrode occurred, resulting in a partial reduction of the top electrode area and a sudden decrease in the current density. For the Pt and Ti–Au electrode, better adherence of the electrodes to the alumina films was achieved; therefore, electrode lift-off was less serious in these structures.

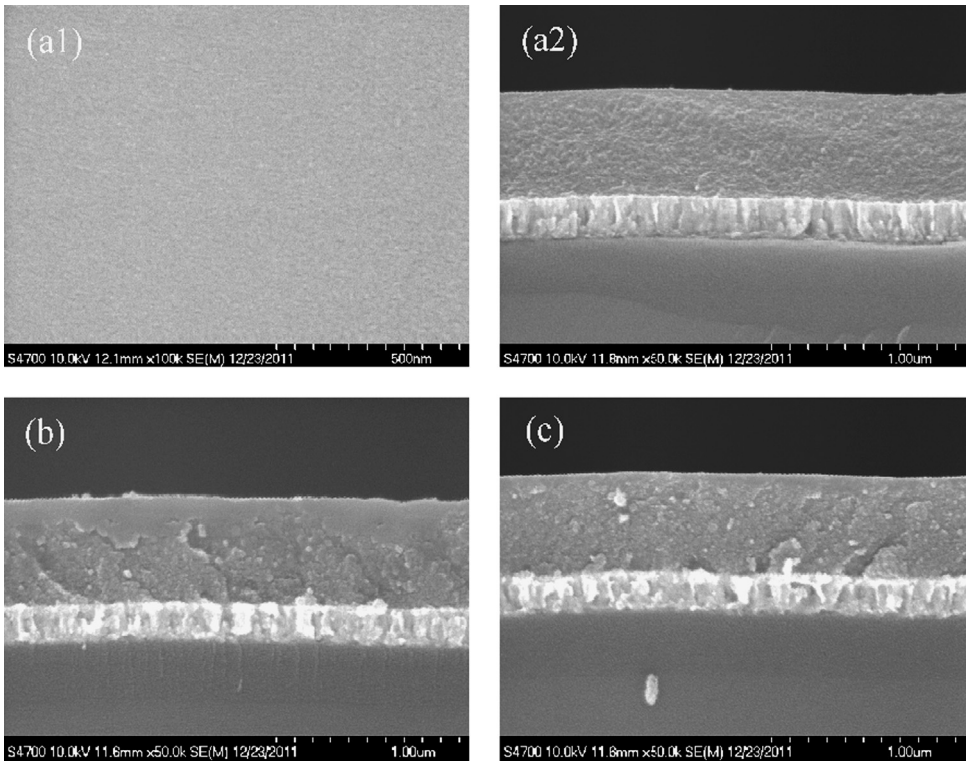

Fig. 5. FESEM micrographs of Al_2O_3 films treated at: (a1) 550 °C, surface; (a2) 550 °C, cross-section; (b) 600 °C, cross section; (c) 650 °C, cross-section.

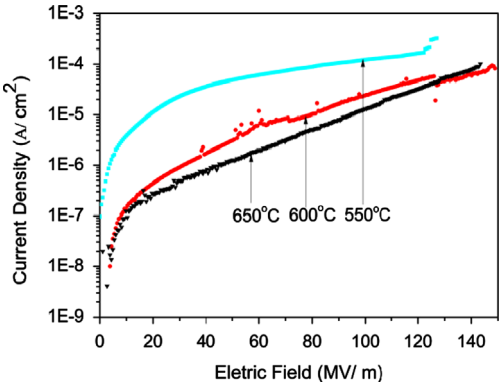

Fig. 6. Current density vs. electric field of Al_2O_3 films calcined at 550 °C, 600 °C and 650 °C.

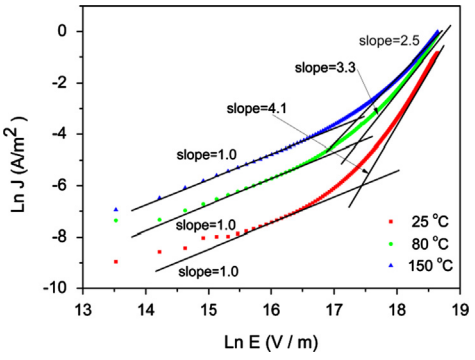

Fig. 7. ln J vs. ln E curves of Al_2O_3 thin film at temperatures ranging from 25 °C to 150 °C.

In general, the top electrode material has a profound effect on the leakage current. Fig. 8 shows that the ionization energy of the top-electrode material has an evident effect on the leakage current of the films. The smaller the ionization energy is, the higher the current density will be. The ionization energies of the top-electrode materials are given in Table 1.

It is possible that the metal atoms of the capacitor anode can be ionized under an electric field. The resulting cations can be moved from the anode into the amorphous alumina film, where many unoccupied cation sites are available [27], these sites favor the diffusion of such cations through thin films. The diffusion tail can act as a conductive path in thin oxide films [25,28]. The Ti atoms can be ionized more easily due to the lower ionization energy, and more Ti ions will diffuse into the thin film. Thus, the leakage current of the capacitor with a Ti top electrode was the highest among the three MIM structure.

We then investigated the dielectric properties of the Al_2O_3 films calcined at various temperatures. Figs. 9 and 10 show the capacitance, dielectric constant and dielectric loss of the films in an electric field, respectively. Fig. 9 shows that the capacitance of the film capacitors fell in the range of 75–90 pF. As the calcination temperature increased from 550 °C to 650 °C, the capacitance decreased from 87 pF to 79 pF. All three capacitors were very stable with respect to the applied voltage. The dielectric constant and dielectric loss were calculated from the capacitance. The film calcined at 550 °C showed the highest dielectric constant of 7.4. As the calcination temperature increased to 650 °C, the dielectric constant decreased to the lowest value of 6.7. The variation in the dielectric constant is consistent with the results of Vitanov

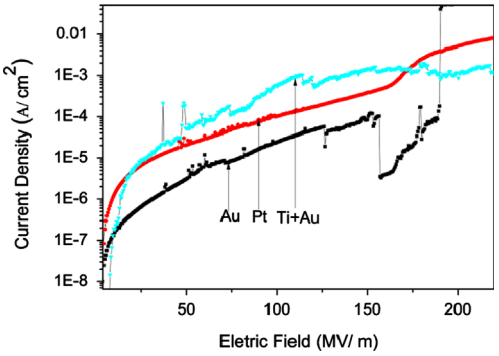

Fig. 8. *J–E* plot for Al_2O_3 films calcined at 600 °C with Au, Ti+Au and Pt top electrodes.

Table 1
The first ionization energy of various metal atoms.

Metal atom	Ti	Pt	Au
Ionization energy (eV)	6.828	9.000	9.226

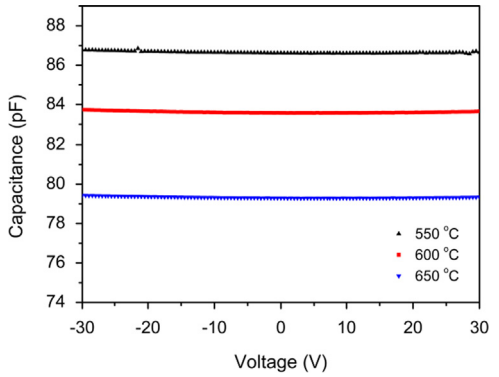

Fig. 9. Capacitance vs. voltage of the Al_2O_3 film capacitors calcined at various temperatures ($f=10^4$ Hz).

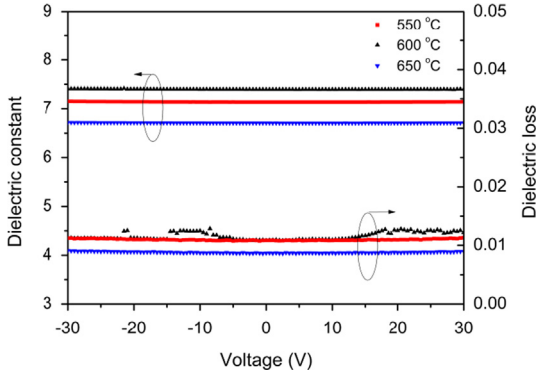

Fig. 10. Dielectric constant and loss vs. electric voltage of the Al_2O_3 film capacitors calcined at various temperatures ($f=10^4$ Hz).

et al. [21]. The leakage current is one of the major factors contributing to the dielectric loss. The film calcined at 650 °C showed the lowest dielectric loss of 0.009, which is consistent with the fact that the film showed the lowest leakage current.

4. Conclusions

Crack-free and homogeneous alumina films were successfully prepared by sol–gel and spin-coating methods. The XRD results show that the thin films were amorphous. No extra elements were observed in the XPS spectra, except for a low amount of carbon. The leakage current density decreased with the increase in calcination temperature from 550 °C to 650 °C. The leakage current showed a linear dependence on voltage in the low-electric-field region. This result is indicative of ohmic conduction. At higher electric fields, the current density ascends to higher values due to the effect of space charges. The ionization energy of the top-electrode material clearly affected the leakage current of the Al_2O_3 MIM capacitors. The dielectric constants of the Al_2O_3 films calcined at 550 °C, 600 °C and 650 °C were approximately 7.4, 7.2 and 6.7, respectively; the corresponding dielectric losses were 0.012, 0.011 and 0.009, respectively.

Acknowledgments

This research was partially supported by the National Science Foundation of China under Contract no. 51272177 and the Science and Technology Commission of Shanghai Municipal under Contract no. 11ZR1439700.

References

[1] J.L. Sun, C.X. Liu, X.H. Zhang, B.W. Wang, X.Y. Ni, Effect of diopside addition on sintering and mechanical properties of alumina, Ceramics International 35 (4) (2009) 1321–1325.
[2] I. Piwoński, K. Soliwoda, The effect of ceramic nanoparticles on tribological properties of alumina sol–gel thin coatings, Ceramics International 36 (1) (2010) 47–54.
[3] K. Vanbesien, P. De Visschere, P. Smet, D. Poelman, Electrical properties of Al_2O_3films for TFEL-devices made with sol–gel technology, Thin Solid Films 514 (1) (2006) 323–328.
[4] H. Kim, T. Troczynski, Thick alumina dielectric films on aluminum through chemically bonded composite sol–gel, Ceramics International 33 (3) (2007) 333–336.
[5] N. Ozer, J.P. Cronin, Y.J. Yao, A.P. Tomsia, Optical properties of sol–gel deposited Al_2O_3 films, Solar Energy Materials and Solar Cells 59 (4) (1999) 355–366.
[6] T. Ishizaka, Y. Kurokawa, Optical properties of rare-earth ion (Gd^{+3}, Ho^{+3}, Pr^{+3}, Sm^{+3}, Dy^{+3} and Tm^{+3})-doped alumina films prepared by the sol–gel method, Journal of Luminescence 92 (2001) 57–63.
[7] W. Lee, R. Ji, U. Gösele, K. Nielsch, Fast fabrication of long-range ordered porous alumina membranes by hard anodization, Nature Materials 5 (9) (2006) 741–747.
[8] W. Hu, D. Gong, Z. Chen, L. Yuan, K. Saito, C.A. Grimes, P. Kichambare, Growth of well-aligned carbon nanotube arrays on silicon substrates using porous alumina film as a nanotemplate, Applied Physics Letters 79 (19) (2001) 3083–3085.
[9] P. Katiyar, C. Jin, R. Narayan, Electrical properties of amorphous aluminum oxide thin films, Acta Materialia 53 (9) (2005) 2617–2622.
[10] W. Koh, S.J. Ku, Y. Kim, Chemical vapor deposition of Al_2O_3 films using highly volatile single sources, Thin Solid Films 304 (1) (1997) 222–224.
[11] T. Maruyama, T. Nakai, Aluminum oxide thin films prepared by chemical vapor deposition from aluminum 2-ethylhexanoate, Applied Physics Letters 58 (19) (1991) 2079–2080.

[12] M. Aguilar-Frutis, M. Garcia, C. Falcony, G. Plesch, S. Jimenez-Sandoval, A study of the dielectric characteristics of aluminum oxide thin films deposited by spray pyrolysis from Al $(acac)_3$, Thin Solid Films 389 (1) (2001) 200–206.
[13] S. Maniv, W. Westwood, Discharge characteristics for magnetron sputtering of Al in Ar and Ar/O_2 mixtures, Journal of Vacuum Science and Technology 17 (3) (1980) 743–751.
[14] C. Jing, X. Zhao, Y. Zhang, Sol–gel fabrication of compact, crack-free alumina film, Materials Research Bulletin 42 (4) (2007) 600–608.
[15] Q. Fu, C.B. Cao, H.S. Zhu, Preparation of alumina films from a new sol–gel route, Thin Solid Films 348 (1) (1999) 99–102.
[16] T. Olding, M. Sayer, D. Barrow, Ceramic sol–gel composite coatings for electrical insulation, Thin Solid Films 398 (2001) 581–586.
[17] K. Murali, P. Thirumoorthy, Characteristics of sol–gel deposited alumina films, Journal of Alloys and Compounds 500 (1) (2010) 93–95.
[18] C. Krug, E. Da Rosa, R. De Almeida, J. Morais, I. Baumvol, T. Salgado, F. Stedile, Atomic transport and chemical stability during annealing of ultrathin Al_2O_3 films on Si, Physical Review Letters 85 (19) (2000) 4120–4123.
[19] W. Zhang, W. Liu, C. Wang, Characterization and tribological investigation of sol–gel Al_2O_3 and doped Al_2O_3 films, Journal of the European Ceramic Society 22 (16) (2002) 2869–2876.
[20] H. Bartzsch, D. Glöß, B. Böcher, P. Frach, K. Goedicke, Properties of SiO_2 and Al_2O_3 films for electrical insulation applications deposited by reactive pulse magnetron sputtering, Surface & Coatings Technology 174 (2003) 774–778.
[21] P. Vitanov, A. Harizanova, T. Ivanova, T. Dimitrova, Chemical deposition of Al_2O_3 thin films on Si substrates, Thin Solid Films 517 (23) (2009) 6327–6330.
[22] E.C. Onyiriuka, Aluminum, titanium boride, and nitride films sputter-deposited from multicomponent alloy targets studied by XPS, Applied Spectroscopy 47 (1) (1993) 35–37.
[23] D. Leinen, A. Fernandez, J. Espinos, J. Holgado, A. González-Elipe, An XPS study of the mixing effects induced by ion bombardment in composite oxides, Applied Surface Science 68 (4) (1993) 453–459.
[24] A. Lim, A. Atrens, ESCA studies of nitrogen-containing stainless steels, Applied Physics A: Materials Science & Processing 51 (5) (1990) 411–418.
[25] G. Yip, J. Qiu, W. Ng, Z. Lu, Effect of metal contacts on the electrical characteristics of Al_2O_3 dielectric thin films, Applied Physics Letters 92 (2008) 122911.
[26] N. Klein, The mechanism of self-healing electrical breakdown in MOS structures, IEEE Transactions on Electron Devices 13 (11) (1966) 788–805.
[27] R.M. Handy, Electrode effects on aluminum oxide tunnel junctions, Physical Review 126 (6) (1962) 1968.
[28] R.H. Doremus, Diffusion in alumina, Journal of Applied Physics 100 (10) (2006) 101301–101317.